THE JOURNAL OF PROSTHETIC DENTISTRY

RESEARCH AND EDUCATION

Dynamic nature of abutment screw retightening: Finite element study of the effect of retightening on the settling effect

Haddad Arabi Bulaqi, MSc,[a] Mahmoud Mousavi Mashhadi, PhD,[b] Hamed Safari, DDS, MS,[c] Mohammad Mahdi Samandari, MSc,[a] and Farideh Geramipanah, DDS, MS[d]

ABSTRACT

Statement of problem. A fundamental problem in fully understanding the dynamic nature of screw loosening is lack of recognition of the entire process of screw tightening and retightening.

Purpose. The purpose of this study was to explain the dynamic nature of abutment screw retightening by using finite element methods to investigate the effect of the coefficient of friction and retightening on the settling effect.

Material and methods. Precise computer models were designed of a Straumann dental implant, a directly attached crown, an abutment screw, and the bone surrounding the implant. All threaded interfaces were designed with a spiral thread helix with a specific coefficient of static and kinetic friction, and the surfaces were characterized as fine, regular, and rough. Abaqus software was used for dynamic simulation, which involved applying rotational displacement to the abutment screw and torque controlling during the steps of tightening, relaxation, retightening, and second relaxation and at different coefficients of friction. The obtained torque and preload values were compared to the predicted values.

Results. When surfaces changed from fine to rough, the remaining torque and preload decreased, and the settling effect increased. Upon retightening, the remaining torque and preload increased, and the settling effect also decreased.

Conclusions. The reduction of the coefficient of friction contributes to increases in the preload and decreases in the settling effect. Retightening reduced the settling effect and had an insignificant effect on the preload. At high coefficients of friction, the retightening effect was intensified. (J Prosthet Dent 2015;113:412-419)

A dental implant is a prosthetic replacement for a missing tooth and consists of an implant, an abutment, and an overlying crown or other dental prosthesis. The most common method to secure the abutment to the implant is a retaining screw. Some common complications associated with this type of retaining system are screw loosening and fracture,[1-3] particularly with single-tooth restorations[4,5] and external hexagonal connection systems.[6,7] The prevalence of screw loosening is about 38% in external hexagonal systems.[8,9] In fact, 26% of gold prosthesis-retaining screws and 43% of abutment screws loosen during the first year of service.[8,10]

Two methods are used to prevent screw loosening: sufficient preload[11-13] and antirotational resistance form.[14,15] Improvements in the design of the implant-abutment junction have led to a significant reduction in the incidence of screw loosening. These modifications involve the addition of antirotational designs. Examples include larger external hexagons, frictional fit abutments, including taper integrated screwed-in abutments and tapered interference fit connections, and the Spline implant.[7,16]

Previous research has demonstrated that preload creates a strong compressive clamping force that keeps the different components tightly connected.[12,17] The preload and clamping force are equal but in opposite

[a]Graduate student, Department of Mechanical Engineering, School of Mechanics, University of Tehran, Tehran, Iran.
[b]Professor, Department of Mechanical Engineering, School of Mechanics, University of Tehran, Tehran, Iran.
[c]Assistant Professor, Department of Periodontics, School of Dentistry, Qom University of Medical Sciences, Qom, Iran.
[d]Associate Professor, Implant Research Center, Department of Prosthodontics, School of Dentistry, Tehran University of Medical Sciences, Tehran, Iran.

Clinical Implications

A full understanding of the mechanism of screw loosening can help clinicians to implement appropriate avoidance measures. The settling effect plays an important role in screw loosening. Retightening the screw a few minutes after the initial tightening can reduce this effect.

directions. Preload is defined as the tensile force built in the axial axis of the screw; this tensile force is distributed in a nonlinear manner as a result of screw elongation.[11,18] Preload is dependent on the applied torque, the component material, the screw head and thread design, and the coefficient of friction for the contact surfaces.[18,19] The coefficient of friction can be reduced with lubrication and an increased rate of tightening; in contrast, it can be increased by increasing material hardness and surface roughness.[20]

The uniform pressure theory can be used to calculate the sliding friction of the conical interface, which is similar to the cone clutch. According to this theory, the pressure distribution is uniform in the radial direction of the conical surface. Budynas and Nisbett[21] proposed Equation (1) to determine the frictional resistance of the thread torque (T_{th}) and Equation (2) to determine the conical torque (T_c). Additionally, wrench torque (T_w, Eq. (3)) is the sum of the thread and conical torques.

$$T_{th}=\frac{d_m}{2}\times\frac{L+(\mu\times\pi\times d_m\times\sec\alpha)}{(\pi\times d_m)-(\mu\times L\times\sec\alpha)}\times F=K_{th}\times F \quad (1)$$

$$T_c=\frac{\mu}{3\sin\beta}\times\frac{D^3-d^3}{D^2-d^2}\times F=K_c\times F \quad (2)$$

$$T_w=T_{th}+T_c=[K_{th}+K_c]\times F \quad (3)$$

$$T_{th\text{-}w}=\frac{T_{th}}{T_w}=\frac{K_{th}}{K_{th}+K_c} \quad (4)$$

$$P=\frac{T_w}{K_{th}+K_c}=\frac{35}{K_{th}+K_c}, \quad (5)$$

where $T_{th\text{-}w}$ represents the ratio of thread torque to wrench torque. In addition, F is the preload created in the screw; P is the preload at the recommended torque of 35 Ncm; μ is the coefficient of friction in the threads and

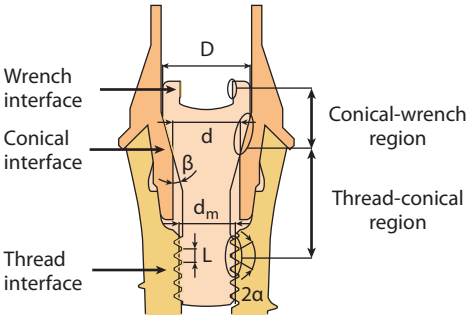

Figure 1. Geometric parameters of implant complex; d=2.015 mm, D=2.6 mm, α=2β=π/6 radian, L=0.4 mm, d_m=1.66 mm.

conical head; d is the inner head friction diameter; D is the outer head friction diameter; β is the cone angle head; α is the half angle of the thread; L the is pitch length; and d_m is the pitch diameter. The geometric parameters are presented in Figure 1.

In a 6-year follow-up study, Haas et al[22] showed that the use of high tightening torque could reduce the incidence of screw loosening. Stüker et al[23] demonstrated that generated preloads on gold screws using a dry lubricant were 3 times greater than those on titanium screws.

Excessive bending at the screw joint and the settling effect, otherwise known as embedment relaxation, also contribute to screw loosening.[7,11,12] The settling effect is based on the fact that no surface is completely smooth. This microroughness prevents the 2 surfaces from fully contacting each other. Once the initial torque is applied, the rough spots are the only surfaces that remain in contact. However, these contact spots flatten as a result of the highly concentrated pressure. Consequently, micromovement occurs in the opposite direction of the elongation axis of the screw, thereby resulting in a loss of preload.[24] This loss can be as high as 2% to 10%.[25] The 3 major parameters that influence the settling effect are initial surface roughness, surface hardness, and magnitude of preload.[11] Winkler et al[24] concluded that in order to reduce the settling effect, the abutment screw should be retightened 10 minutes after the initial torque is applied. As previously mentioned, roughness and hardness are 2 parameters that influence the coefficient of friction.[20] Therefore, an increase in the coefficient of friction and preload will likely lead to an increase in the settling effect.[11]

Regarding the implant-abutment interface design, Aboyoussef et al[7] observed that abutments that had an improved resistance design reduced the incidence of screw loosening due to an increase in the moment arm, which is defined as the length from the center of rotation of the screw interface to the crown/abutment interface. However, variation in the coefficient of friction can

influence the mechanical behavior of screw tightening. In a study conducted by Tzenakis et al,[26] salivary contamination and repeated retightening of the screw caused a higher preload as a result of a reduction in friction. Likewise, Hagiwara[27] observed that friction was reduced with repeated tightening of the screw compared to a single tightening of the screw. Farina et al[28] evaluated tightening techniques used in an implant-supported denture set and concluded that the use of the retorque application significantly increased joint stability.

Another factor that must be considered is the mechanism of preload loosening over time. Cantwell and Hobkirk[29] observed that the greatest and most rapid preload changes occur in the first 2 seconds. They also found that the decrease in preload is an exponential function over the long term. Indeed, the mean preload loss over the first 15 hours was 24.9%; however, 29.5% of this loss occurred within the first 2 seconds, and 40.2% occurred within the first 10 seconds.

Several in vitro and in vivo studies have attempted to explain the mechanisms involved in the screw-tightening procedure. However, a detailed description of the different steps involved in this procedure (tightening, relaxation, and retightening) is still lacking, probably because of the complex and unconventional experimental procedure required to elucidate this information. The finite element method offers the ability to gather and study elaborate data that cannot be obtained by using conventional methods. In this study, finite element methods were used to explain the dynamic nature of screw retightening and the effect of the coefficient of friction and retightening on the settling effect throughout the different steps associated with tightening the abutment screw in a dental implant.

MATERIAL AND METHODS

For a complete simulation with proper boundary conditions, a mandibular posterior section was modeled by using cone beam computed tomography, and CATIA V5 R19 (Dassault Systèmes) software was used to create computer-aided design (CAD) files. Note that this mandibular section contained a central trabecular core surrounded by a dense cortical layer.

The geometry models of a Straumann implant (SLA 043.031S; Institute Straumann), a directly attached crown (048.642, RN SynOcta gold abutment), and an abutment screw (048.356, SynOcta basal screw) were constructed with a projection microscope and SOLIDWORKS (Dassault Systèmes) software. The diameter of the implant was 4.1 mm, and the length was 8 mm. In order to simulate the process of screw tightening, preload creation, and osseointegration, the exact geometry of the abutment screw and implant threads were modeled. The outer surfaces of the implant and abutment screw were geometrically modeled with a continuous spiral threaded helix, and the inner surfaces of the implant and bone bore were geometrically modeled with a continuous spiral threaded bore. The thread pitch of the abutment screw was 0.4 mm, and the thread pitch of the implant was 1.25 mm.

All material properties were considered to be isotropic and homogeneous. The mechanical behavior of the implant component materials was assumed to be both elastic and plastic. Also, the mechanical properties of the surrounding bone were assumed to be linear and elastic. Table 1 presents the mechanical properties of the materials used.[30]

The coulomb friction and penalty method were used to model the dry friction contact for the abutment screw, abutment, and fixture. In order to compare the qualitative and quantitative effects of the surface character, 3 different types of friction conditions were considered. Specifically, 3 coefficients of kinetic friction (μ_k), 0.12 for fine surfaces, 0.16 for regular surfaces, and 0.20 for rough surfaces, were used for the tightening and retightening steps, and 3 coefficients of static friction (μ_s), 0.16 for fine surfaces, 0.20 for regular surfaces, and 0.24 for rough surfaces, were used for the relaxation steps.[12,31] Note that the coefficient of kinetic friction is always lower than that of static friction. The implant-bone interface was assumed to be completely osseointegrated; therefore, the contact of implant-bone interface was defined as "tie." After assembling the implant complex inside the bone, the screw was placed in the "snug-tight" condition, as shown in Figure 2.

For the explicit dynamic simulation, the CAD models were transferred to the ABAQUS 6.11 (Dassault Systèmes Simulia Corp) software. The explicit element library and the free meshing technique with linear geometric order were used to generate the tetrahedral elements. Tangential behavior and contact interface with specific coefficients of friction were defined for the reciprocal contacting surfaces. Table 2 lists the number of elements for the model parts, and Figure 3 shows the meshed models for the fixture, abutment screw, and abutment.

As the abutment screw rotates around its axis one complete turn, it displaces one screw pitch inside the thread of the fixture. The preload is induced by the resistance against the axial displacement and causes elongation in the abutment screw. The simulation was performed in 4 main steps. In step 1 (tightening [t]), using an angular velocity of 0.5 radian per second, the wrench turned the abutment screw enough to achieve a torque of 35 Ncm. In step 2 (the first relaxation [re1]), the wrench was removed for 2 seconds so that the initial relaxation could occur. In step 3 (retightening [rt]), the wrench retightened the abutment screw with an angular velocity of 0.5 radian per second until a torque of 35 Ncm

Table 1. Mechanical properties of model components

Material Component	Young Modulus (GPa)	Poisson Ratio	Density (g/cm^3)	Ultimate Strength (MPa)	Elongation (%)
Gold abutment*	136	0.37	17.5	765	10 min
Titanium grade 4*	110	0.34	4.5	550	15 min
Cortical bone[30]	13.70	0.3	3	190	2 max
Trabecular bone[30]	1.37	0.3	3	10	2 max

*Manufacturer's specifications.

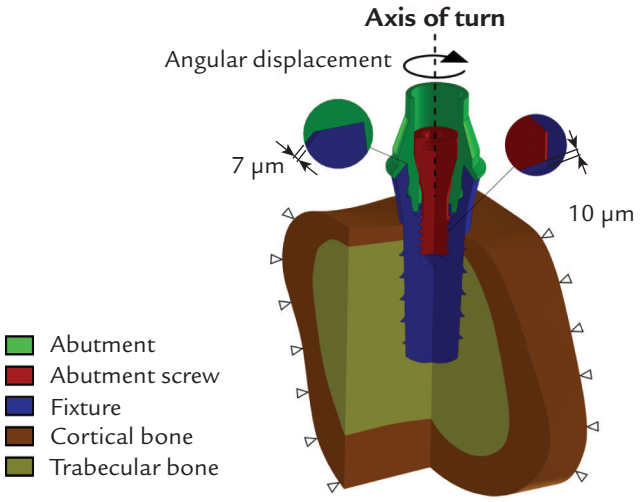

Figure 2. Three-dimensional models of structure. Depicted gaps are in micrometers.

was regained. In step 4 (the second relaxation [re2]), the wrench was completely removed, and the second relaxation occurred over the next 2 seconds.

The relationships among the wrench torque, the conical torque, the thread torque, and the preload were assessed with respect to time for different coefficients of friction. Additionally, linear regression was used to analyze the conical torque, thread torque, and preload data in the second (T_c^{re1},T_{th}^{re1},P_2) and fourth (T_c^{re2},T_{th}^{re2},P_4) steps.

RESULTS

The balance of torques acting on the wrench, conical, and thread interfaces were evaluated in the 4 steps using free body diagrams (Fig. 4). Figure 5 shows the values of wrench torque, conical torque, thread torque, and preload with respect to time for the 4 steps at different friction coefficient values. The maximum created wrench torque in the first (T_w^t) and third (T_w^{rt2}) steps for all surface conditions was 35 Ncm. The values of the conical and thread torques were T_c^t=26 and T_{th}^t=9 Ncm in the first step and T_c^{rt2}=25.77 and T_{th}^{rt2}=9.23 Ncm in the third step (μ_k=0.12).

Table 2. Number of tetrahedral elements for each part in model

Part	No. of Elements
Implant (fixture)	78 774
Abutment screw	32 303
Abutment	24 925
Cortical bone	39 700
Trabecular bone	55 947

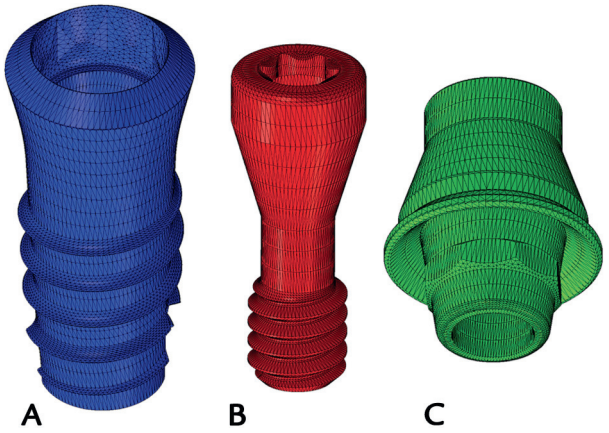

Figure 3. Finite element models. A, Fixture. B, Abutment screw. C, Abutment.

The wrench torque at the second (T_w^{re1}) and fourth (T_w^{re2}) steps were totally dampened after a few vibrations in these steps, and the value of the conical torque (T_c^{re1}, T_c^{re2}) and the thread torque (T_{th}^{re1},T_{th}^{re2}) were equal in the opposite directions. The values of the thread torque were 7.96 Ncm in the second step and 8.18 Ncm in the fourth step (μ_s=0.16). The amounts of wrench torque, conical torque, and thread torque in the 4 steps at the various friction coefficient values are presented in Table 3.

The maximum values of the preload in the first step (P_1) were 504.1 N (μ_k=0.12), 393.1 N (μ_k=0.16), and 319.9 N (μ_k=0.20). The values of the preload in the first (P_1) and third (P_3) steps and the relationship between the preload loosening with respect to time in the second (P_2) and fourth (P_4) steps are presented in Table 4. Figure 6 shows the predicted and simulated values of the ratio of thread torque to wrench torque and the preload as a function of the friction coefficient. The values of these ratios and preload values are shown in Table 5.

DISCUSSION

Screw loosening is considered a major complication associated with dental implants.[3] Changes in the factors considered influential to the preload, such as the antirotational properties of the abutment, the settling effect, and functional loads, may play a fundamental role in screw loosening. According to the mechanics of

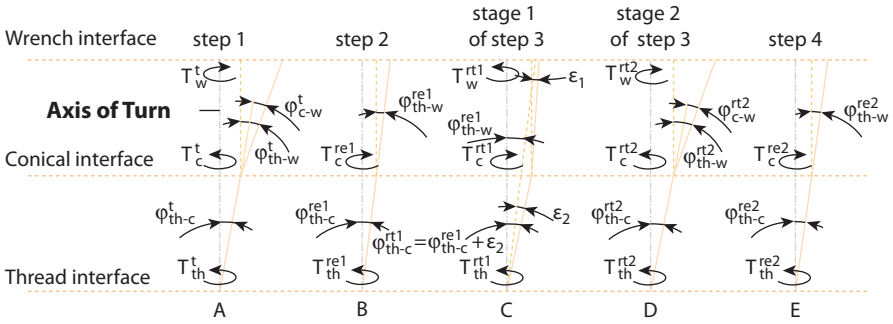

Figure 4. Free body diagrams of abutment screw show corresponding wrench torque (T_w), conical torque (T_c), and thread torque (T_{th}). A, During tightening. B, First relaxation. C, D, Retightening. E, Second relaxation.

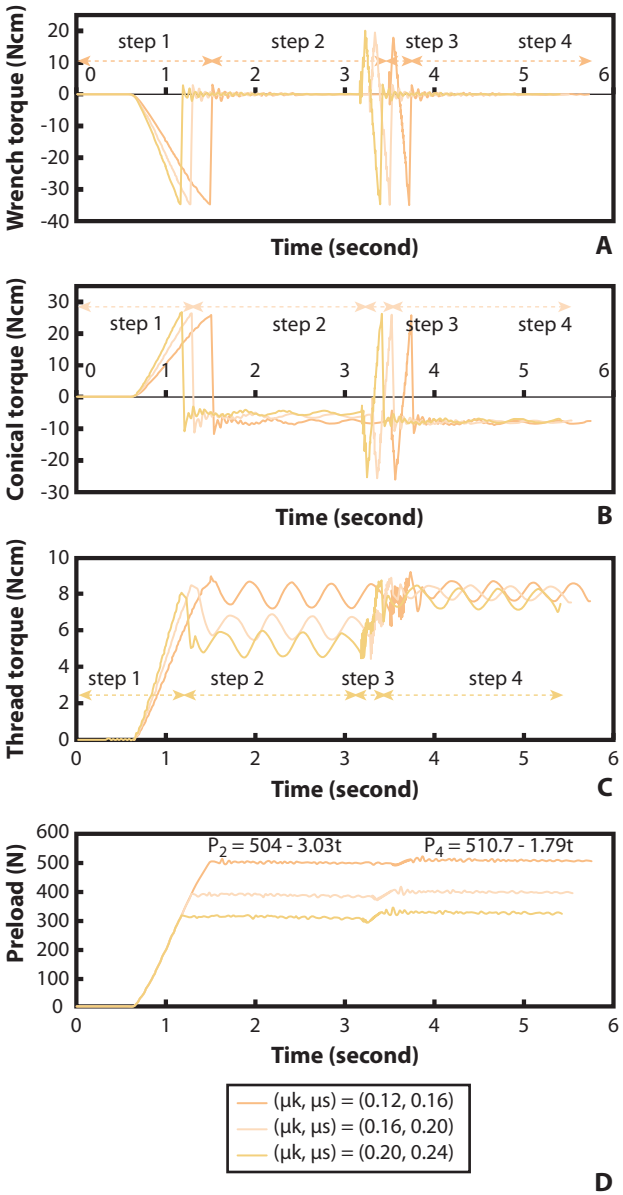

Figure 5. A, Changes in wrench torque (T_w). B, Conical torque (T_c). C, Thread torque (T_{th}). D, Preload (P).

materials, if a shaft with the length L, shear modulus G, and a polar moment of inertia J is twisted by torque T, an angular twist of $\varphi=(T\times L)/(G\times J)$ would be created. Also, note that the angular twist φ is proportional to the applied torque T.[32]

Two contact regions in the abutment screw are defined as the thread-conical and conical-wrench regions (Fig. 1). By applying the rotational displacement to the abutment screw in the first step and regarding the frictional resistance at the conical (T_c^t) and thread (T_{th}^t) interfaces, the wrench torque (T_w^t) is consequently created at the wrench interface (Eq. (6), Fig. 4A).

The angular twist of φ_{th-c}^t at the thread-conical region and φ_{c-w}^t at the conical-wrench region were created by T_{th}^t and T_w^t. By choosing the thread interface as the origin for the coordinates, the angular twist at the conical-thread region was φ_{th-c}^t and at the wrench-thread region was $\varphi_{th-c}^t+\varphi_{c-w}^t$ (Fig. 4A). By removing the wrench in the second step, the angular twist φ_{c-w}^t was also eliminated, and according to the equilibration condition, the thread torque (T_{th}^{re1}) was counterbalanced by the conical torque (T_c^{re1}) (Eq. (7), Fig. 4B). Because the conical portion of the abutment screw and the abutment act as a wedge, the torsional resistance, T_c^t, which is created by tightening, is restored as internal energy (preload), which attempts to push out the abutment screw. In the second step, the restored internal energy is reduced as a result of counterbalancing the magnitude of resistance T_{th}^{re1} while disregarding the negligible damping. The remaining torque (T_c^t-T_{th}^{re1}) is thus distributed at the conical interface.

The third step, retightening, comprised 2 substages. In the first substage, the screw head turns ε_1 radian; note that ε has a very small value. As a result, the remaining restored energy (T_c^t-T_{th}^{re1}) is released at the conical interface and appears as the torsional torque T_c^{rt1}. This behavior indicates that the ε_2 radian turn, which occurs at the conical interface, was in the same direction as ε_1 such that $\varepsilon_2>\varepsilon_1$. Therefore, the torque at the wrench interface (T_w^{rt1}) has a positive value and increases until

Table 3. Values of wrench torque (T_w), conical torque (T_c), and thread torque (T_{th}) in 4 steps of tightening, first relaxation, retightening, and second relaxation and with various friction coefficients (Ncm)

Coefficients of Friction (μ_k, μ_s)	Step 1		Step 2	Step 3				Step 4
	T_c^t	T_{th}^t	T_c^{re1}=-T_{th}^{re1}	T_c^{rt1}	T_w^{rt1}	T_c^{rt2}	T_{th}^{rt2}	T_c^{re2}=-T_{th}^{re2}
(0.12, 0.16)	26	9	-7.96	-26.10	-18.14	25.77	9.23	-8.18
(0.16, 0.20)	26.51	8.49	-6.22	-25.87	-19.65	26.11	8.89	-8.09
(0.20, 0.24)	26.90	8.10	-5.3	-25.45	-20.15	26.25	8.75	-7.77

μ_k, coefficient of kinetic friction; μ_s, coefficient of static friction.

Table 4. Values of preload (*P*) in 4 steps with different friction coefficients (N)

Coefficients of Friction (μ_k, μ_s)	Step 1 P_1	Step 2 $P_2=P_1-(b_1 \times t)$	Step 3 P_3	Step 4 $P_4=P_3-(b_2 \times t)$
(0.12, 0.16)	504	P_2=504.0-3.03t	510.7	P_4=510.7-1.97t
(0.16, 0.20)	393.1	P_2=393.1-4.75t	401.8	P_4=401.8-2.13t
(0.20, 0.24)	319.9	P_2=319.9-5.74t	330.6	P_4=330.6-2.26t

reaching the value of T_c^{rt1} (Eq. (8), Fig. 4C). In substage 2 of step 3, the wrench torque (T_w^{rt2}) decreased to -35 Ncm with the increase in the angle of the turn (Eq. (9), Fig. 4D). In step 4, the wrench is removed again, and the relaxation mechanism of the second step is repeated (Eq. (10), Fig. 4E).

$$T_w^t = T_{th}^t + T_c^t \quad (6)$$

$$T_c^{re1} = -T_{th}^{re1} \quad (7)$$

$$T_c^{rt1} = T_w^{rt1} + T_{th}^{rt1} \quad (8)$$

$$T_w^{rt2} = T_c^{rt2} + T_{th}^{rt2} \quad (9)$$

$$T_c^{re2} = -T_{th}^{re2} \quad (10)$$

Using saliva as a wet lubricant[26] and gold-coated surfaces as a dry lubricant,[29] the preload increased because of the resulting reduction in the coefficient of friction. Additionally, the studies conducted by Tzenakis et al[26] and Hagiwara[27] demonstrated that the coefficient of friction reduced with retightening. The reduction in preload after tightening the screw is a function of time. Cantwell and Hobkirk[29] described the following 3 factors that reduce preload after tightening: torsional relaxation, embedment relaxation, and localized plastic deformation at the contact surfaces. Furthermore, in the specific implant complex, the factors that influence the settling effect and consequently screw loosening are the preload, the coefficient of friction, and retightening.

With the increase of the friction coefficient, the magnitudes of T_c^t and T_{th}^t also increase, thereby implying that the recommended torque of 35 Ncm is achieved at a lower turn angle; therefore, less elongation occurs in the abutment screw. By reducing the elongation, the preload or the elastic energy stored within the screw decreases, and screw loosening occurs much earlier and with lower external loads (Fig. 5). This fact was predicted by Budynas and Nisbett[21] in Eq. (5) (Fig. 6). According to the predicted values (Eq. (4)) and the data acquired through simulation, the ratio of thread torque to wrench torque reduced with an increase in the coefficient of friction (Fig. 6, Table 5). Additionally, T_{th}^{re1} at the relaxation step is related to the values of T_{th}^t and P_1 at the first step. Therefore, an increase in the friction coefficient reduced

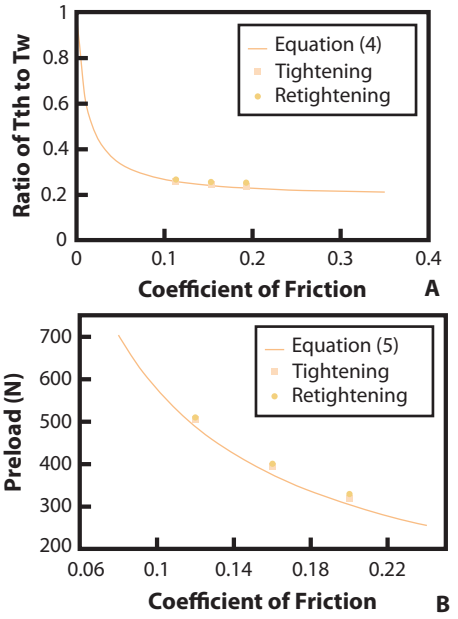

Figure 6. Comparison of predicted and simulated values. A, Ratio of T_{th} to T_w. B, Preload.

Table 5. Predicted and simulated values for ratio of thread torque to wrench torque and preload at different coefficients of kinetic friction

Coefficients of Friction μ_k	Simulated		Predicted	
	Ratio of T_{th}^t to T_w^t	Ratio of T_{th}^{rt2} to T_w^{rt2}	Ratio of T_{th} to T_w (T_{th-w})	Preload (N)
0.12	0.257	0.264	0.252	489
0.16	0.242	0.254	0.236	375
0.20	0.231	0.250	0.225	304

the values of T^{t}_{th} and P_1; consequently, the magnitude of T^{re1}_{th} was reduced. An increase in the friction coefficient resulted in a more significant decrease in T^{re1}_{th}, indicating that T^{t}_{th} - T^{re1}_{th} increased. Consequently, the rate of preload decrease b_1 increased, and the settling effect intensified (Tables 3, 4). Additionally, the settling effect increased the incidence of the screw loosening rate.

As a result of the high contact pressure, the microroughness is smoothed, and the micromovement occurring in the opposite direction of the elongation leads to a decrease in the preload.[24] The preload reduction in the first 2 seconds after the first tightening can be assumed to be approximately linear, even though the preload decreases as an exponential function over the long term.[29] Furthermore, the abrasion of the tips found in areas of microroughness reduces the coefficient of friction by decreasing the surface roughness.

According to the predicted (Eq. (4), Eq. (5)) and simulated data, the use of retightening, which reestablishes the initial applied torque, increased the magnitude of the thread torque and the preload, (T^{rt1}_{th}<T^{rt2}_{th}) (P_3>P_1), (Tables 3, 4). Budynas and Nisbett[21] proved that an increase in the friction coefficient is the main reason for increasing the magnitude of the ratio of thread torque to wrench torque and the preload (Fig. 6).

Because T^{re2}_{th} at the second relaxation step is related to T^{rt2}_{th} and P_3 at the third step, T^{re2}_{th} increases by increasing T^{rt2}_{th} and P_3. An increase in the torque (T_c=-T_{th}) at the relaxation step causes more resistance against loosening or "back off," thereby resulting in a slower preload reduction rate (b_2). This means that the torsional relaxation and the settling effect are reduced and joint stability is increased (Tables 3, 4).[28]

A comparison of the data presented in Tables 3 and 4 reveals that increasing the friction coefficient results in an increase in the rate of T^{re}_{th} and P increases with retightening. Therefore, at greater levels of friction, T^{re2}_{th}-T^{re1}_{th} and P_3-P_1 increase because of the higher influence of the settling effect at higher friction coefficients. Consequently, through retightening, b_1-b_2 increases, and the more settling effect is counterbalanced on surfaces with higher coefficients of friction. This finding is clinically important because the reduction of the coefficient of friction and the settling effect reduces the incidence of screw loosening.[28]

CONCLUSIONS

With wrench removal, torque remains only in the thread-conical region. The preload and the magnitude of the remaining torque in the relaxation step are reduced when the friction coefficient increases, and hence more settling effect accrues. The magnitude of the remaining torque in the thread-conical region increases with retightening. Additionally, retightening reduces the friction coefficient and slightly magnifies the preload increases, thereby reducing the settling effect to a great extent. The effect of retightening is greater with higher friction coefficients.

REFERENCES

1. Pjetursson BE, Bragger U, Lang NP, Zwahlen M. Comparison of survival and complication rates of tooth-supported fixed dental prostheses (FDPs) and implant-supported FDPs and single crowns (SCs). Clin Oral Implants Res 2007;18(suppl 3):97-113.
2. Pjetursson BE, Tan K, Lang NP, Bragger U, Egger M, Zwahlen M. A systematic review of the survival and complication rates of fixed partial dentures (FPDs) after an observation period of at least 5 years. Clin Oral Implants Res 2004;15:667-76.
3. Wittneben JG, Buser D, Salvi GE, Burgin W, Hicklin S, Bragger U. Complication and failure rates with implant-supported fixed dental prostheses and single crowns: a 10-year retrospective study. Clin Implant Dent Relat Res 2014;16:356-64.
4. Goodacre CJ, Kan JY, Rungcharassaeng K. Clinical complications of osseointegrated implants. J Prosthet Dent 1999;81:537-52.
5. Schwarz MS. Mechanical complications of dental implants. Clin Oral Implants Res 2000;11(suppl 1):156-8.
6. Henry PJ, Laney WR, Jemt T, Harris D, Krogh PH, Polizzi G, et al. Osseointegrated implants for single-tooth replacement: a prospective 5-year multicenter study. Int J Oral Maxillofac Implants 1996;11:450-5.
7. Aboyoussef H, Weiner S, Ehrenberg D. Effect of an antirotation resistance form on screw loosening for single implant-supported crowns. J Prosthet Dent 2000;83:450-5.
8. Jemt T, Laney WR, Harris D, Henry PJ, Krogh PH Jr, Polizzi G, et al. Osseointegrated implants for single tooth replacement: a 1-year report from a multicenter prospective study. Int J Oral Maxillofac Implants 1991;6:29-36.
9. Norton MR. An in vitro evaluation of the strength of an internal conical interface compared to a butt joint interface in implant design. Clin Oral Implants Res 1997;8:290-8.
10. Jemt T. Failures and complications in 391 consecutively inserted fixed prostheses supported by Branemark implants in edentulous jaws: a study of treatment from the time of prosthesis placement to the first annual checkup. Int J Oral Maxillofac Implants 1991;6:270-6.
11. Jorneus L, Jemt T, Carlsson L. Loads and designs of screw joints for single crowns supported by osseointegrated implants. Int J Oral Maxillofac Implants 1992;7:353-9.
12. Haack JE, Sakaguchi RL, Sun T, Coffey JP. Elongation and preload stress in dental implant abutment screws. Int J Oral Maxillofac Implants 1995;10:529-36.
13. Jaarda MJ, Razzoog ME, Gratton DG. Effect of preload torque on the ultimate tensile strength of implant prosthetic retaining screws. Implant Dent 1994;3:17-21.
14. Binon PP, McHugh MJ. The effect of eliminating implant/abutment rotational misfit on screw joint stability. Int J Prosthodont 1996;9:511-9.
15. Binon PP. The effect of implant/abutment hexagonal misfit on screw joint stability. Int J Prosthodont 1996;9:149-60.
16. Bozkaya D, Muftu S. Mechanics of the taper integrated screwed-in (TIS) abutments used in dental implants. J Biomech 2005;38:87-97.
17. Patterson EA, Johns RB. Theoretical analysis of the fatigue life of fixture screws in osseointegrated dental implants. Int J Oral Maxillofac Implants 1992;7:26-33.
18. Khraisat A, Hashimoto A, Nomura S, Miyakawa O. Effect of lateral cyclic loading on abutment screw loosening of an external hexagon implant system. J Prosthet Dent 2004;91:326-34.
19. Jorn D, Kohorst P, Besdo S, Rucker M, Stiesch M, Borchers L. Influence of lubricant on screw preload and stresses in a finite element model for a dental implant. J Prosthet Dent 2014;112:340-8.
20. Burguete RL, Johns RB, King T, Patterson EA. Tightening characteristics for screwed joints in osseointegrated dental implants. J Prosthet Dent 1994;71:592-9.
21. Budynas RG, Nisbett JK. Shigley's mechanical engineering design. 9th ed. New York: McGraw-Hill; 2011. p. 414-8. 845-55.
22. Haas R, Mensdorff-Pouilly N, Mailath G, Watzek G. Branemark single tooth implants: a preliminary report of 76 implants. J Prosthet Dent 1995;73:274-9.
23. Stüker RA, Teixeira ER, Beck JC, da Costa NP. Preload and torque removal evaluation of three different abutment screws for single standing implant restorations. J Appl Oral Sci 2008;16:55-8.
24. Winkler S, Ring K, Ring JD, Boberick KG. Implant screw mechanics and the settling effect: overview. J Oral Implantol 2003;29:242-5.
25. Sakaguchi RL, Borgersen SE. Nonlinear contact analysis of preload in dental implant screws. Int J Oral Maxillofac Implants 1995;10:295-302.
26. Tzenakis GK, Nagy WW, Fournelle RA, Dhuru VB. The effect of repeated torque and salivary contamination on the preload of slotted gold implant prosthetic screws. J Prosthet Dent 2002;88:183-91.

27. Hagiwara M, Ohashi N. A new tightening technique for threaded fastners. J Offshore Mech Arct Eng 1994;116:64-9.
28. Farina AP, Spazzin AO, Consani RL, Mesquita MF. Screw joint stability after the application of retorque in implant-supported dentures under simulated masticatory conditions. J Prosthet Dent 2014;111:499-504.
29. Cantwell A, Hobkirk JA. Preload loss in gold prosthesis-retaining screws as a function of time. Int J Oral Maxillofac Implants 2004;19:124-32.
30. Borchers L, Reichart P. Three-dimensional stress distribution around a dental implant at different stages of interface development. J Dent Res 1983;62:155-9.
31. Bowden FP, Tabor D. The friction and lubrication of solids. Oxford: Clarendon Press; 1986.
32. Beer FP. Mechanics of materials. 6th ed. New York: McGraw-Hill; 2011. p. 142-62.

Corresponding author:
Haddad Arabi Bulaqi
School of Mechanics
University of Tehran
North Amir-Abad, Tehran
IRAN
Email: haddad.arabi@ut.ac.ir

Acknowledgment
The authors thank the Amirkabir University of Technology's high-performance computing research center (HPCRC) for computing support of this research.

Copyright © 2015 by the Editorial Council for *The Journal of Prosthetic Dentistry.*

Availability of Journal Back Issues

As a service to our subscribers, copies of back issues of *The Journal of Prosthetic Dentistry* for the preceding 5 years are maintained and are available for purchase from Elsevier, Inc until inventory is depleted. Please write to Elsevier, Inc, Subscription Customer Service, 6277 Sea Harbor Dr, Orlando, FL 32887, or call 800-654-2452 or 407-345-4000 for information on availability of particular issues and prices.